The TIME-Pilot Intensity Mapping Experiment

A.T. Crites[a], J.J. Bock[a], C.M. Bradford[d], T.C. Chang[c], A.R. Cooray[e], L. Duband[f], Y. Gong[e], S. Hailey-Dunsheath[a], J.Hunacek[a], P.M. Koch[c], C.T. Li[c], R.C. O'Brient[a], T. Prouve[f], E. Shirokoff[b], M.B. Silva[g], Z. Staniszewski[a], B. Uzgil[g], M. Zemcov[a]

[a] California Institute of Technology, Pasadena, CA 91125, USA

[b] University of Chicago, Chicago, IL 60637, USA

[c] Institute of Astronomy and Astrophysics, Taipei, Taiwan

[d] Jet Propulsion Laboratory, Pasadena, CA 91109

[e] University of California at Irvine, Irvine, CA 92607

[f] CEA, Grenoble, France

[g] CENTRA, Lisboa, Portugal

[g] University of Pennsylvania, Philadelphia, PA 19104

ABSTRACT

TIME-Pilot is designed to make measurements from the Epoch of Reionization (EoR), when the first stars and galaxies formed and ionized the intergalactic medium. This will be done via measurements of the redshifted 157.7 um line of singly ionized carbon ([CII]). In particular, TIME-Pilot will produce the first detection of [CII] clustering fluctuations, a signal proportional to the integrated [CII] intensity, summed over all EoR galaxies. TIME-Pilot is thus sensitive to the emission from dwarf galaxies, thought to be responsible for the balance of ionizing UV photons, that will be difficult to detect individually with JWST and ALMA. A detection of [CII] clustering fluctuations would validate current theoretical estimates of the [CII] line as a new cosmological observable, opening the door for a new generation of instruments with advanced technology spectroscopic array focal planes that will map [CII] fluctuations to probe the EoR history of star formation, bubble size, and ionization state. Additionally, TIME-Pilot will produce high signal-to-noise measurements of CO clustering fluctuations, which trace the role of molecular gas in star-forming galaxies at redshifts $0 < z < 2$. With its unique atmospheric noise mitigation, TIME-Pilot also significantly improves sensitivity for measuring the kinetic Sunyaev-Zel'dovich (kSZ) effect in galaxy clusters. TIME-Pilot will employ a linear array of spectrometers, each consisting of a parallel-plate diffraction grating. The spectrometer bandwidth covers 185-323 GHz to both probe the entire redshift range of interest and to include channels at the edges of the band for atmospheric noise mitigation. We illuminate the telescope with f/3 horns, which balances the desire to both couple to the sky with the best efficiency per beam, and to pack a large number of horns into the fixed field of view. Feedhorns couple radiation to the waveguide spectrometer gratings. Each spectrometer grating has 190 facets and provides resolving power above 100. At this resolution, the longest dimension of the grating is 31 cm, which allows us to stack gratings in two blocks (one for each polarization) of 16 within a single cryostat, providing a 1x16 array of beams in a 14 arcminute field of view. Direct absorber TES sensors sit at the output of the grating on six linear facets over the output arc, allowing us to package and read out the detectors as arrays in a modular manner. The 1840 detectors will be read out with the NIST time-domain-multiplexing (TDM) scheme and cooled to a base temperature of 250 mK with a 3He sorption refrigerator. We present preliminary designs for the TIME-Pilot cryogenics, spectrometers, bolometers, and optics.

Keywords: reionization, mm-wavelenghts, spectrometers

Send correspondence to A.T. Crites: E-mail: acrites@caltech.edu

Millimeter, Submillimeter, and Far-Infrared Detectors and Instrumentation for Astronomy VII, edited by Wayne S. Holland, Jonas Zmuidzinas, Proc. of SPIE Vol. 9153, 91531W · © 2014 SPIE · CCC code: 0277-786X/14/$18 · doi: 10.1117/12.2057207

1. INTRODUCTION

The period between 200 Myr and 1 Gyr after the Big Bang ($6 < z < 20$) when the first stars and galaxies ionized the intergalactic medium (IGM) is known as the epoch of reionization (EoR). Reionization occurred when early objects produced enough Lyman-continuum photons ($h\nu > 13.6\,\mathrm{eV}$) to ionize the surrounding hydrogen gas.[1,2] Detecting these galaxies which are responsible for reionization is difficult, so the specifics of this period of cosmic history are largely unknown.

Measurements which can access the entire luminosity function of reionizing sources are needed to probe this region of cosmic history. It is possible to probe the sources of reionization and their impact on the IGM by studies of the fluctuations in 3-D tomographic intensity mapping datasets which targets one or more spectral line. This technique is unique because it provides 3-D spatial and spectral information, which allows an integrated measurement of faint galaxies along the line of sight.

The spectral information made available by the TIME-pilot experiment will permit the detection of [CII] the most energetic emission line in galaxies for $\lambda_{\mathrm{rest}} > 40\,\mu$m (Fig.1). Measurements of [CII] are also valuable as a complement to HI 21-cm line intensity mapping,[3–5] which trace the neutral medium at z>6 (e.g. PAPER, MWA, LOFAR). As new HI measurements are made, [CII] data cubes can also be cross-correlated with these new data for key systematic checks. By measuring [CII] TIME-Pilot provides a vital stepping stone towards understanding the epoch of reionization.

2. SCIENCE GOALS

TIME-pilot will accomplish three science goals. The primary goal is to intensity map the [CII] fluctuations. Additionally TIME-pilot will measure the integrated CO from intermediate-redshift galaxies and measure the kSZ signal from clusters of galaxies using an auxiliary 150 GHz channel.

2.1 Intensity Mapping [CII] Fluctuations

[CII] measurements target emission from galaxies during the EoR. This is in contrast with typical 21-cm EoR intensity mapping experiments which target neutral hydrogen in the ISM. Using [CII] to study the EoR is a sensible choice because of carbon's abundance in the Universe and its uniquely low ionization energy (11.3 eV, lower than hydrogen). This extremely low ionization energy allows diffuse starlight to easily ionize it, so carbon is typically present in the ISM in its singly ionized state. The [CII] line is one of the brightest spectral lines in aggregate spectra of star-forming galaxies: it makes up 0.1 percent to 1 percent of the total IR luminosity.[6,7] It has been widely detected, including in high redshift galaxies, some $z > 6$ galaxies, and quasars.[8–11] It is also detectable using earth-based telescopes because of its convenient redshift into the relatively transparent 1.2 mm atmospheric window (195-310 GHz) for TIME-Pilot's target redshift range of $5 < z < 9$.

2.2 CO Measurements

TIME-*Pilot* observations will also measure CO intensity fluctuations from intermediate redshift galaxies, which act as a foreground and must be subtracted for [CII] EoR measurements. Two models, the Sargent et al. (2012) model[12] and the Obreschkow et al. (2009) model, are used to estimate the masking required to CO power subdominant to the [CII] power. The Sargent et al. (2009) model uses a prescription similar to that in Carilli & Walter (2013)[13] and indicates that masking to a depth of $3{\times}10^{-22}\,\mathrm{W\,m^{-2}}$ is sufficient, as shown by Fig. 2, and will require the removal of ∼28% of the total survey volume. The more conservative Obreschkow et al. (2009) model estimates less CO emission than the Sargent et al. (2012) model, and requires substantially less masking. The details of this masking analysis will be pioneered once we have first measurements from TIME-*Pilot* and the CO levels are more well-known.

In addition to providing measurements of the level of foreground emission that must be masked, the CO data measure the spatial distribution and abundance of molecular gas in galaxies. This is an interesting astrophysics measurement, since molecular gas is the fuel for star formation and TIME-*Pilot* will be measuring it during a broad range of cosmic time that includes the peak epoch of star formation at $z \sim 2$. The majority of observations of high redshift molecular gas have been obtained in galaxies selected for their high star-formation rates,(e.g., SFR $\geq 100\ M_\odot\,\mathrm{yr}^{-1}$ at $z = 0.2 - 1.0$[14] and SFR $\geq 30\ M_\odot\,\mathrm{yr}^{-1}$ at $z = 1.0 - 2.5$[15]). However, an unbiased search

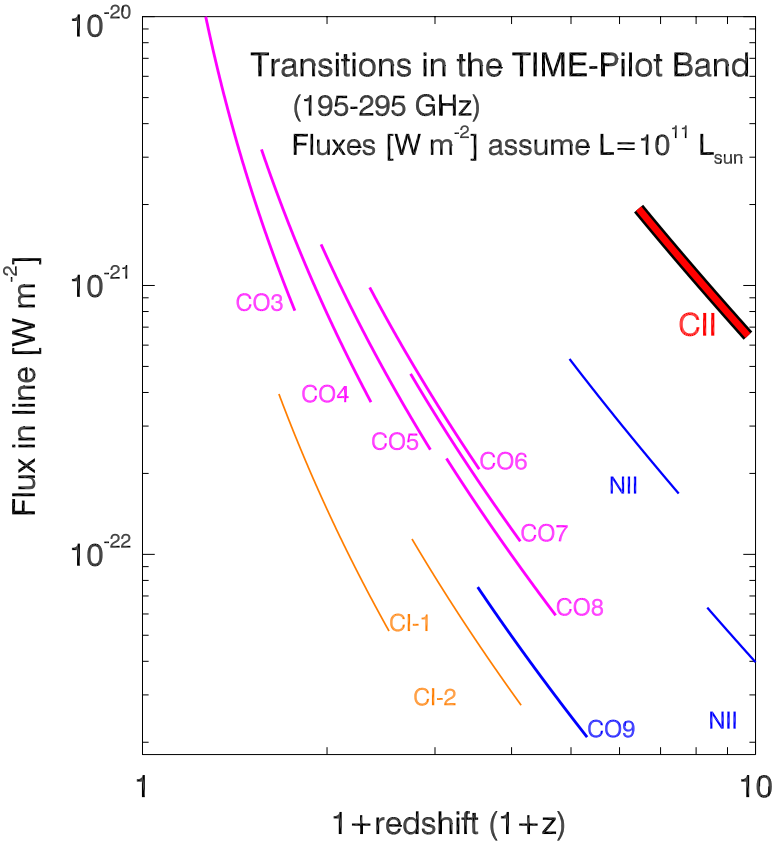

Figure 1. Typical galactic spectral lines redshifted into the TIME-*Pilot* band. The [CII] is dominant in the z=5–9 range which probes the EoR.

for CO emission with sufficient sensitivity to probe gas masses characteristic of the normal star-forming galaxy population is required for a full census of the molecular gas content over time.

2.3 kSZ Measurements

TIME-pilot is also ideally suited to measure the kinetic SZ (kSZ) effect in individual galaxy clusters, as the kSZ effect peaks in the TIME-pilot spectral band. Measurements of the kSZ effect provide a direct, redshift-independent measurement of the velocity field of galaxy clusters, because the kSZ effect is caused by the motion of a galaxy cluster with respect to the CMB.[16] The cosmological large-scale velocities yielded by this measurement provide an important complement to other cosmological probes, but the small surface brightness of the kSZ effect makes it a difficult measurement to make.

Broad-band kSZ measurements are limited by atmospheric noise, so TIME-pilot's ability to spectrally remove atmospheric emission results provides a unique advantage over current instruments. We estimate that TIME-pilot's kSZ sensitivity will be 10-fold greater than current instrument, based on measured atmospheric and instrument noise levels in the Bolocam and MUSIC,[17] along with atmospheric noise models. TIME-Pilot will also obtain longer wavelength information for cluster spectral studies using 16 broad band photometer channels at 150 GHz, and this will allow separation of the tSZ and kSZ effects. A short line scan will be used to observe clusters in order to keep pixels on and off the cluster at all times.

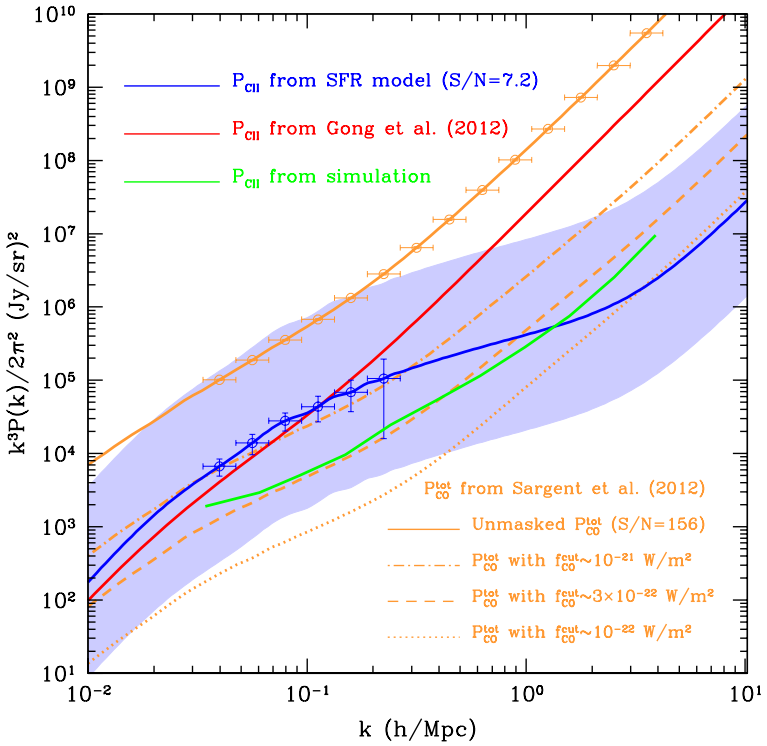

Figure 2. 3-D auto-correlation power spectra of EoR [CII] and intermediate-z CO in the TIME-Pilot band. Red, blue, and green curves mark [CII] power from the 'High,' 'SFR', and 'Millennium' estimates, respectively, described in the text. The tan-colored lines show power in CO: the upper curve includes all the CO-emitting galaxies, the lower broken curves show the power after masking to various depths.

3. CRYOGENIC AND MECHANICAL DESIGN

TIME-*Pilot* will use an existing closed-cycle cryostat (Fig. 3). The cryostat is cooled with a Cryomech PT-415 4 K refrigerator which provides a base temperature < 4 K. It also includes two custom lower-temperature stages: a recirculating ^{4}He system for 1 K and a ^{3}He dual sorption system for 300 mK. A second ^{3}He stage which will cool the gratings and detectors to a stable 250 mK. We will add a 300 mK enclosure around the spectrometers and high-permeability magnetic shielding. The 4 K stage will provide the cold stop at a pupil, and the 1 K stage will house the final polyethylene reimaging lens.

4. OPTICS

TIME-*Pilot* will couple to the telescope using relay optics that form an image of the primary mirror inside the cryostat, and a 4K cold stop will be installed at this location to reduce stray light. The beam is converted by a cold (1K) high density polyethylene lens, with a porous teflon AR coating, to a telecentric $f/3$ focus. A set of metal-mesh low-pass edge (LPE) filters and dielectric blocking filters will be used to reduce the optical loading on the 300 mK stages, while a metal-mesh LPE combined with the feedhorn will define the bandpass.

5. SPECTROMETERS

TIME-*Pilot* will measure 3-D fluctuations created by [CII] emission in galaxies from $5 < z < 9$, using 32 independent single-beam, single-polarization spectrometers, as showing in Fig. 3 and Table 1, and described in

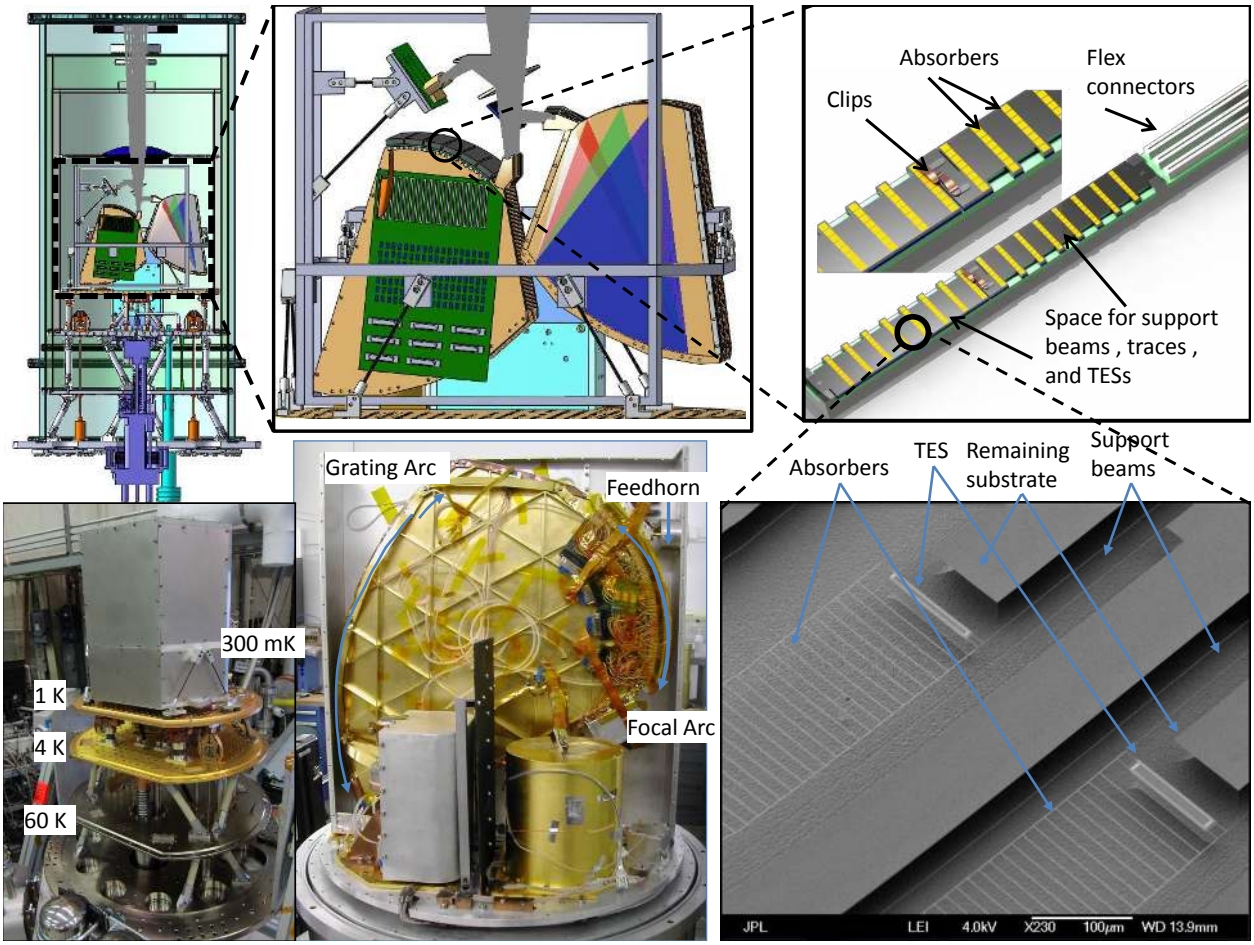

Figure 3. The TIME-*Pilot* Instrument The instrument will be housed in a closed-cycle 4 K–1 K–300 mK cryostat (bottom left), with an enlarged cryogenic volume to allow insertion of the spectrometer stacks and optics (top left). The 32 waveguide grating spectrometers are assembled into two stacks of 16, they couple the same 1-D linear field on the sky via a polarizing grid (top center). Each grating spectrometer is similar to that used in Z-Spec (bottom center), but they are smaller and simpler for TIME-*Pilot* since they operate at lower resolving power (R=150, vs. R=300 for Z-Spec). The dispersed light is detected with twelve 2-D arrays of TES bolometers which span the spectrometer stacks (right) with a total of 1840 detectors. The TESes are similar to those built at JPL for CMB polarimetry as well as more demanding (lower-background) spectroscopic applications. Sixteen 150 GHz broadband channels view the same sky as the spectrometers via a dichroic filter, and will be used for precise measurements of the kinetic SZ effect in galaxy clusters.

detail below. The spectrometers are arrayed in two stacks of 16, one stack for each polarization. The input feeds for both stacks are arranged to couple to the same line on the sky via a polarizing grid. The feed spacing is $2.2\,f\lambda$, giving a total 1-D field-of-view of $13.6'$. We emphasize that all TIME-*Pilot* key technologies have been demonstrated in scientific applications. Measuring the low-k modes sensitive to clustering (see Fig. 2) requires simultaneous wide-band spectral and wide-field spatial coverage. The spectral bandwidth is provided naturally with our spectrometer, but we also target coverage on angular scales $\sim 1^\circ$. TIME-*Pilot* uses an observing strategy that optimizes the S/N needed to detect the amplitude of the [CII] clustering signal on large spatial scales. We find the optimal solution is a concentrated line scan that is 156×1 beams = $1.3^\circ \times 0.5'$ on the sky.

Instantaneous wide-band spectral coverage with background-limited sensitivity requires a diffraction grating spectrometer. Fabry-Perot and Fourier-Transform systems have penalties for scanning and excess noise, respectively. This once presented a problem, since conventional slit-fed echelle grating spectrometers are too large and bulky in the millimeter band. However, we have pioneered a unique approach using a curved grating in

Table 1. TIME-*Pilot* Experiment Parameters

Number of spectrometers	32, 16 each pol, grid diplexed
Number of photometers	16, spectrally diplexed
Total # of detectors	1840
Instantaneous FOV	13.6 arcmin × 0.5 arcmin
Final $f/\#$	$f/3.3$, after relay optics + cold lens
Cryostat	Existing 4K / 1K closed-cycle cryostat
Base temperature	250 mK via ^{3}He cooler
C+ Survey field size	78 arcmin × 0.5 arcmin rectangle
C+ Survey on-sky integration time	240 hours
tSZ δy sensitivity	$\pm 8.5 \times 10^{-6}$ per beam in 4 hours
kSZ $\delta v_{\rm pec}$ sensitivity	$\pm 250\,{\rm km\ s^{-1}}$ per beam in 4 hours

Instrument Parameters

Parameter	Photometers	Grating LF Band	Grating HF Band
Spectral range [GHz]	135-165	185-240	240-323
Estimated end-to-end optical efficiency	0.3	0.3	0.3
# of Bolometers per sub-band	1	27 (9×3)	30 (10×3)
# of Bolometers	16	864	960
$\nu/\delta\nu$ per bolometer	5	93–116	89–112
NEI on sky $[({\rm MJy/sr})\sqrt{\rm sec}]$	0.3	$2.1 - 3.2$	$3.2 - 5.0$
NEFD on sky $[{\rm mJy}\sqrt{\rm sec}]$	14	$60 - 70$	$60 - 70$

TES Bolometer Parameters

Ti TES T_C for sky [mK]	450	450	450
Al TES T_C for lab [mK]	1200	1200	1200
TES safety factor	3	3	3
Thermal conductance G at T_C [pW/K]	140	8	12
Detector + MUX NEP $[10^{-18}\,{\rm W\,Hz^{-1/2}}]$	40	9	11
Photon NEP $[10^{-18}\,{\rm W\,Hz^{-1/2}}]$	60	12–15	15–20
Absorber size [mm]	ϕ 4.0	3.0 × 1.7	3.0 × 2.6

parallel-plate waveguide which both focuses and diffracts the broadband light from a single waveguide mode (e.g. from a feedhorn) to a detector array.[18,19] This approach dramatically decreases the total volume of the spectrometer; it has been used in Z-Spec at R=300, a single-beam predecessor to TIME-*Pilot*, and in R=700 prototypes developed for higher frequency space and balloon applications (see Fig. 4).

Each spectrometer is a simple machined, bolted aluminum assembly. The spectrometers require global tolerances of $\lambda/10$ ($\sim 100\,\mu$m for our application) for the waveguide plates. Low surface roughness that is required for the plates is obtained by lapping. We note that in these previous applications, we have already demonstrated operation with higher resolving power and/or tighter tolerances than required for TIME-*Pilot*. We have developed a preliminary design for the TIME-*Pilot* grating shown in Fig. 3. It has 190 facets and provides resolving power of the 140–200, ensuring that detector sampling exceeds the resolving power, and its longest dimension is 31 cm. The output arc is approximated by 6 linear facets, so that when the spectrometers are stacked in the two groups of 16, each stack creates 6 planes, each 2 cm×14 cm on which the 2-D detector arrays will be mounted.

6. DETECTORS

TIME-*Pilot* will use arrays of silicon-nitride leg-isolated, superconducting transition edge sensor (TES) bolometers. A total of 1840 detector will be used for TIME-pilot. The detector technology used in TIME-pilot shares approaches with current CMB experiment from Catech/JPL including: 1) the use of the elemental titanium thermistor with $T_C = 450$ mK providing a steep transition and large loop gain, 2) operation from a 250 mK base temperature, 3) use of a second aluminum ($T_C \sim 1$K) thermistor that functions under higher background for laboratory characterization, and 4) use of the NIST SQUID time-domain multiplexer (TDM) and UBC multi-channel readout electronics (MCE).

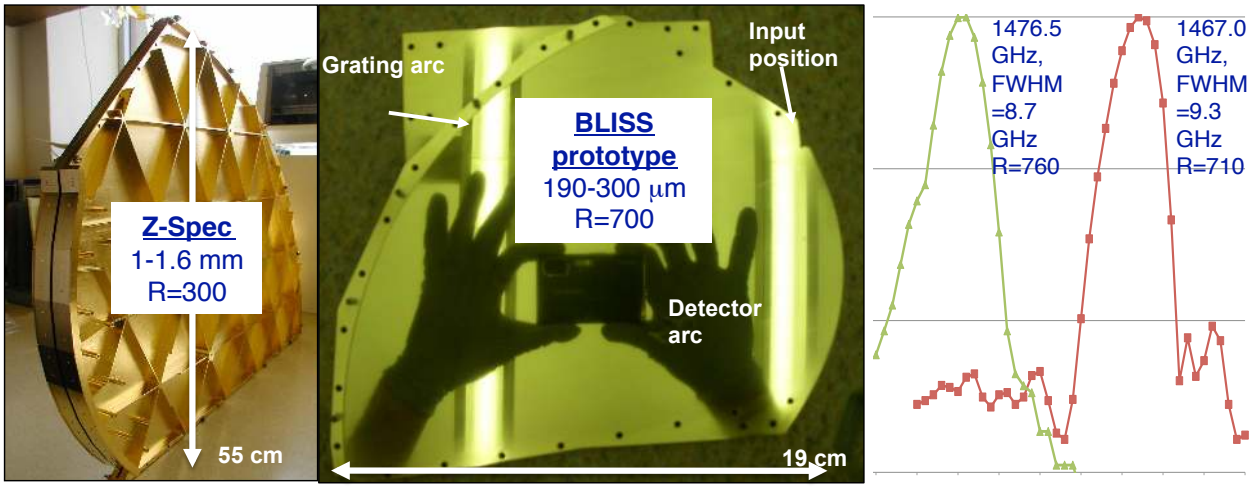

Figure 4. TIME-*Pilot* waveguide spectrometer technology. *Left:* Spectrometer with 481 grating facets used in the Z-Spec instrument. It provides R=300 across the 1 mm atmospheric window (0.95–1.65 mm; 182–316 GHz). *Center* is a R=700 far-IR prototype, much more demanding than the TIME-*Pilot* spectrometers, with a 981-facet grating for 182–303 μm (the top plate is removed). *Right:* Measured spectral profiles of this far-IR grating at two nearby frequencies using a local oscillator source and a scanned output feed coupling a 4 K bolometer. The horizontal axis is position on the output arc (total range of 2 mm in the plot), and the vertical axis is logarithmic with horizontal lines indicating orders of magnitude. The mapping of frequency to output position, and the resolving power ($R = \nu/\delta\nu_{\rm FWHM} \sim 700$) of the system are as designed. Below shows 4 spectral profiles calculated as part of the TIME-*Pilot* grating design, with Gaussian fits.

Unlike antenna-fed CMB detectors, for TIME-*Pilot* we take the simpler approach of direct absorption on the micromesh (a.k.a. 'spider-web') island as was used in Z-Spec, as well as the Herschel and Planck space missions. A small prototype TIME-*Pilot* array is shown in the bottom right pannel of Fig. 3. With the narrow bandwidth on each detector, TIME-*Pilot* requires somewhat lower noise equivalent power (NEP $\sim 1\times10^{-17}$ W Hz$^{-1/2}$) than has been fielded with TES arrays, but we have demonstrated much lower NEPs than required as part of our JPL program to develop low-background detectors. We have developed a detector design with detailed noise and speed-of-response calculations for TIME-*Pilot* (Table 1).

The 48 detector sub-arrays will be formed on sparsely-filled silicon dies, providing ample room for bolometer legs and wiring, each 7 cm×2 cm. Each die covers 8 stacked spectrometers in one of the grating output planes described above, and will carry 8×9=72 (low-frequency) or 8×10=80 (high-frequency) detectors. Each is bonded to a backshort wafer, as implemented in the Herschel-SPIRE detector arrays. Each array pair will be housed in a single assembly including a printed circuit board and a copper housing which mounts to the spectrometer assembly (see Fig. 3). The array packages will be connected to two large multiplexing circuit boards via superconducting flexi-cable (aluminum traces patterned on kapton) similar to SPIDER CMB focal plane arrays.[20] Calculations for the NEP required for the detectors over the TIME-*Pilot* bandwith have been calculated and are seen in Fig. 5.

7. CONCLUSIONS

The TIME-pilot intensity mapping experiment is an important pathfinder for future experiments using the [CII] line to study the epoch of reionization. We will use existing bolometer and spectrometer technology to deploy TIME-pilot on a short timescale and make a measurement of the [CII] power spectrum. The instrument design and assembly is progressing. Final designs for the spectrometer gratings exist. The masks for the prototype bolometer arrays have been made and fabrication will being in the next couple weeks. Cold electronics for

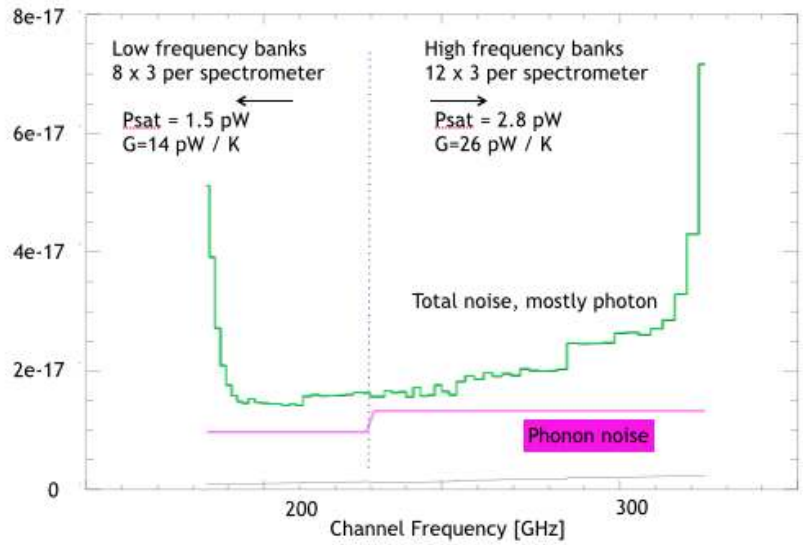

Figure 5. NEP calculations for TIME-pilot detectors. The y-axis is NEP in units of $W/\sqrt{Hz}$.

reading out the detectors and mechanical and thermal structures to support the spectrometers and detectors are currently being designed.

REFERENCES

[1] Becker, G. D., Sargent, W. L. W., Rauch, M., and Calverley, A. P., "High-redshift Metals. II. Probing Reionization Galaxies with Low-ionization Absorption Lines at Redshift Six," *The Astrophysical Journal* **735**, 93 (July 2011).

[2] Spergel, D. N., Bean, R., Doré, O., Nolta, M. R., Bennett, C. L., Dunkley, J., Hinshaw, G., Jarosik, N., Komatsu, E., Page, L., Peiris, H. V., Verde, L., Halpern, M., Hill, R. S., Kogut, A., Limon, M., Meyer, S. S., Odegard, N., Tucker, G. S., Weiland, J. L., Wollack, E., and Wright, E. L., "Three-Year Wilkinson Microwave Anisotropy Probe (WMAP) Observations: Implications for Cosmology," *The Astrophysical Journal Supplement* **170**, 377–408 (June 2007).

[3] Madau, P., Meiksin, A., and Rees, M. J., "21 Centimeter Tomography of the Intergalactic Medium at High Redshift," *The Astrophysical Journal* **475**, 429 (Feb. 1997).

[4] Loeb, A. and Zaldarriaga, M., "Measuring the Small-Scale Power Spectrum of Cosmic Density Fluctuations through 21cm Tomography Prior to the Epoch of Structure Formation," *Physical Review Letters* **92**, 211301 (May 2004).

[5] Gnedin, N. Y. and Shaver, P. A., "Redshifted 21 Centimeter Emission from the Pre-Reionization Era. I. Mean Signal and Linear Fluctuations," *The Astrophysical Journal* **608**, 611–621 (June 2004).

[6] Crawford, M. K., Genzel, R., Townes, C. H., and Watson, D. M., "Far-infrared spectroscopy of galaxies - The 158 micron C(+) line and the energy balance of molecular clouds," *The Astrophysical Journal* **291**, 755–771 (Apr. 1985).

[7] Stacey, G. J., Geis, N., Genzel, R., Lugten, J. B., Poglitsch, A., Sternberg, A., and Townes, C. H., "The 158 micron C II line - A measure of global star formation activity in galaxies," *The Astrophysical Journal* **373**, 423–444 (June 1991).

[8] Boselli, A., Gavazzi, G., Lequeux, J., and Pierini, D., "[CII] at 158 mu m as a star formation tracer in late-type galaxies," *Astronomy and Astrophysics* **385**, 454–463 (Apr. 2002).

[9] Nagamine, K., Wolfe, A. M., and Hernquist, L., "Detectability of [C II] 158 μm Emission from High-Redshift Galaxies: Predictions for ALMA and SPICA," *The Astrophysical Journal* **647**, 60–73 (Aug. 2006).

[10] Stacey, G. J., Hailey-Dunsheath, S., Ferkinhoff, C., Nikola, T., Parshley, S. C., Benford, D. J., Staguhn, J. G., and Fiolet, N., "A 158 μm [C II] Line Survey of Galaxies at z ˜ 1-2: An Indicator of Star Formation in the Early Universe," *The Astrophysical Journal* **724**, 957–974 (Dec. 2010).

[11] de Looze, I., Baes, M., Bendo, G. J., Cortese, L., and Fritz, J., "The reliability of [C II] as an indicator of the star formation rate," *Monthly Notices of the Royal Astronomical Society* **416**, 2712–2724 (Oct. 2011).

[12] Sargent, M. T., Béthermin, M., Daddi, E., and Elbaz, D., "The Contribution of Starbursts and Normal Galaxies to Infrared Luminosity Functions at z $<$ 2," *The Astrophysical Journal Letters* **747**, L31 (Mar. 2012).

[13] Carilli, C. L. and Walter, F., "Cool Gas in High-Redshift Galaxies," *Annual Reviews of Astronomy and Astrophysics* **51**, 105–161 (Aug. 2013).

[14] Combes, F., "Molecular Gas in High Redshift Galaxies," in [*Astronomical Society of the Pacific Conference Series*], Kawabe, R., Kuno, N., and Yamamoto, S., eds., *Astronomical Society of the Pacific Conference Series* **476**, 23 (Oct. 2013).

[15] Tacconi, L. J., Neri, R., Genzel, R., Combes, F., Bolatto, A., Cooper, M. C., Wuyts, S., Bournaud, F., Burkert, A., Comerford, J., Cox, P., Davis, M., Förster Schreiber, N. M., García-Burillo, S., Gracia-Carpio, J., Lutz, D., Naab, T., Newman, S., Omont, A., Saintonge, A., Shapiro Griffin, K., Shapley, A., Sternberg, A., and Weiner, B., "Phibss: Molecular Gas Content and Scaling Relations in z ˜ 1-3 Massive, Main-sequence Star-forming Galaxies," *The Astrophysical Journal* **768**, 74 (May 2013).

[16] Sunyaev, R. A. and Zeldovich, Y. B., "The Observations of Relic Radiation as a Test of the Nature of X-Ray Radiation from the Clusters of Galaxies," *Comments on Astrophysics and Space Physics* **4**, 173 (Nov. 1972).

[17] Sayers, J., Mroczkowski, T., Zemcov, M., Korngut, P., Bock, J., Bulbul, E., Czakon, N., Egami, E., Golwala, S., Koch, P. M., Lin, K.-Y., Mantz, A., Molnar, S. M., Moustakas, L., Pierpaoli, E., Rawle, T. D., Reese, E. D., Rex, M., Shitanishi, J. A., Siegel, A., and Umetsu, K., "A Measurement of the Kinetic Sunyaev-Zel'dovich Signal Towards MAC J0717.5+3745," *The Astrophysical Journal, In Press* (Nov. 2013).

[18] Bradford, C. M., Naylor, B. J., Zmuidzinas, J., Bock, J. J., Gromke, J., Nguyen, H., Dragovan, M., Yun, M., Earle, L., Glenn, J., Matsuhara, H., Ade, P. A. R., and Duband, L., "WaFIRS: A waveguide far-IR spectrometer: Enabling spectroscopy of high-z galaxies in the far-IR and submillimeter," in [*IR Space Telescopes and Instruments*], Mather, J. C., ed., **4850**, 1137–1148 (Mar. 2003).

[19] Bradford, C. M., Kenyon, M., Holmes, W., Bock, J., and Koch, T., "Sensitive far-IR survey spectroscopy: BLISS for SPICA," in [*Society of Photo-Optical Instrumentation Engineers (SPIE) Conference Series*], *Presented at the Society of Photo-Optical Instrumentation Engineers (SPIE) Conference* **7020** (Aug. 2008).

[20] Runyan, M. C., Ade, P. A. R., Amiri, M., Benton, S., Bihary, R., Bock, J. J., Bond, J. R., Bonetti, J. A., Bryan, S. A., Chiang, H. C., Contaldi, C. R., Crill, B. P., Dore, O., O'Dea, D., Farhang, M., Filippini, J. P., Fissel, L., Gandilo, N., Golwala, S. R., Gudmundsson, J. E., Hasselfield, M., Halpern, M., Hilton, G., Holmes, W., Hristov, V. V., Irwin, K. D., Jones, W. C., Kuo, C. L., MacTavish, C. J., Mason, P. V., Morford, T. A., Montroy, T. E., Netterfield, C. B., Rahlin, A. S., Reintsema, C. D., Ruhl, J. E., Schenker, M. A., Shariff, J., Soler, J. D., Trangsrud, A., Tucker, R. S., Tucker, C. E., and Turner, A., "Design and performance of the SPIDER instrument," in [*Society of Photo-Optical Instrumentation Engineers (SPIE) Conference Series*], *Society of Photo-Optical Instrumentation Engineers (SPIE) Conference Series* **7741** (July 2010).